Solution-Processable All-Solid-State Chloride-Selective Electrode: Enhanced Sensitivity from Anion Dopant Exchange

Shi Hoe Ng,[a,†] Georgina E.K.K. Seah[a, †,*] Dorsasadat Safanama,[a] and Shermin S. Goh[a,*]

[a] Institute of Materials Research and Engineering (IMRE), Agency for Science, Technology and Research (A*STAR), 2 Fusionopolis Way, Innovis #08-03, Singapore 138634, Republic of Singapore

***Corresponding authors:**
Georgina Seah georgina-seah@imre.a-star.edu.sg
Shermin S. Goh gohsms@imre.a-star.edu.sg
† These authors contributed equally to this work.

ABSTRACT:
Ion-selective electrodes (ISEs) are widely used in many industries, with recent research focusing on their miniaturization by replacing the liquid filling solutions with solid-contacts. Solution-processing is the preferred method for preparing solid-contact ISEs (SC-ISEs) due to its ease and scalability. However, while there are many solution-processable cationic SC-ISEs, this remains a challenge for anionic SC-ISEs due to poorer compatibility with the solid-contacts. Many anionic SC-ISEs are still prepared by complex techniques, such as electropolymerisation of the solid-contact. Thus, strategies for solution-processable solid-contacts which can interface well with anionic ion-selective membrane (ISMs) are required. Here, we report the fabrication of a fully-solution-processable chloride (Cl^-) SC-ISE by anion exchange of poly(3,4-ethylenedioxythiophene)-polyethylene glycol (PEDOT-PEG) solid-contact before drop-casting the ISM. Significant improvement in sensitivity was observed after PEDOT-PEG anion exchange, with the optimal SC-ISE exhibiting near-Nernstian response (−53.3 ± 0.5 mV/decade, versus −33.4 ± 1.8 mV/decade for the unexchanged SC-ISE) across a wide dynamic range (0.05 M to 6.03 μM). Our SC-ISE also exhibited excellent selectivity against phosphate ($H_2PO_4^-$), bicarbonate (HCO_3^-) and acetate ($CH_3CO_2^-$) and could also be utilized with minimal conditioning time and for prolonged usage. Finally, given the importance of Cl^- sensing in healthcare, we also demonstrated the potential of our Cl^- SC-ISE in sensing multiple synthetic biological samples such as sweat, urine and blood, and real human sweat (forearm samples). This work not only demonstrates the versatility of our anion exchange protocol, but also furthers the understanding of the different enhancement mechanisms – sensitivity or selectivity – depending on whether an ionophore was present in the ISM. We showed that regardless of the mechanism, our simple and efficient protocol could mitigate the issue of the original underperformance and can thus be readily extended to the scalable preparation of multiple types of anion-selective SC-ISEs.

Keywords: ion-selective electrode, ion sensor, chloride, solid contact, conducting polymer, transduction layer

Chloride (Cl^-) sensing is instrumental in various industries such as environmental monitoring, food safety and healthcare. In healthcare, chloride concentration in saliva and sweat is used as an essential biomarker for the diagnosis of cystic fibrosis.[1–3] Blood and urine chloride levels can also be used as an indicator for detection of hyperchloremia and hypochloremia, which signals disease relating to the kidneys,[4] heart,[5] or liver.[6,7] Given the clinical relevance of the Cl^- anion, several research groups have developed potentiometric wearable sensors for sweat Cl^- detection. Most of these sensors are based on silver-silver chloride (Ag|AgCl) electrodes.[8–11] Although these electrodes are easy to fabricate, AgCl is corrosive to the skin, and can easily tarnish in environments with low Cl^- concentration. In contrast, polymeric membrane-based ion-selective electrodes (ISEs) offer better skin compatibility and flexibility.[12,13] Solid-contact ISEs (SC-ISEs) are the miniaturised, planar and all-solid-state progenies of traditional liquid-

filled ISEs.[14,15] They have been widely integrated into wearables in recent years due to their convenience, low cost, and quick analysis time.[16,17] While there are many cationic SC-ISEs such as potassium [18–20] and calcium,[16,19] anionic SC-ISEs are less common, presumably due to poorer compatibility with the solid-contacts.[21,22] Of the limited examples of Cl^- SC-ISEs,[23–28] almost all require tedious processes such as electropolymerisation[29] or interfacial polymerisation for fabrication of the solid-contact.

Solution-processing is currently the method of choice for preparing SC-ISEs due to its ease and scalability.[15] In our recent work, we reported fully solution-processable nitrate (NO_3^-) SC-ISEs,[22,30] fabricated simply by drop-casting poly(3,4-ethylenedioxythiophene)-polyethylene glycol (PEDOT-PEG) onto the electrode, followed by anion exchange, and finally drop-casting of the ion-selective membrane (ISM). Electrochemical and spectroscopic investigations showed that the PEDOT-PEG:ClO_4 dispersion (Sigma-Aldrich) contained excessive amounts of perchlorate (ClO_4^-) dopant, which hindered the transport of NO_3^- anions. The ion exchange protocol replaced the ClO_4^- dopant of PEDOT-PEG with NO_3^- anion, eliminating the additional diffusion-limited resistance, resulting in enhanced **selectivity** performance.

Herein, to demonstrate further the advantages of our newly reported protocol, we focused on the fabrication of Cl^- SC-ISEs. Unexpectedly, we found that the dopant species had a direct effect on the **sensitivity** of the Cl^- SC-ISE, with the anion exchange step necessary to achieve a near-Nernstian response towards Cl^- and elucidated the different mechanisms of enhancement. Additionally, as both the ISM and the solid-contact of the SC-ISE contained the Cl^- anion, it could be used with minimal conditioning, which saves preparation time. Finally, we demonstrated the potential healthcare applications for these all-solid-state Cl^- SC-ISEs using various synthetic and real human samples.

MATERIALS AND METHODS

Materials. PEDOT-PEG, 0.8 wt% dispersion in propylene carbonate (contains ClO_4^- as dopant, PEDOT-PEG:ClO_4), high molecular weight poly(vinyl chloride) (PVC), chloride ionophore IV (5-bis-[*N*-(butyl)thioureido]-2,7-di-*tert*-butyl-9,9-dimethylxanthene), tridodecylmethylammonium chloride (TDMA*Cl*), 1-(2-nitrophenoxy)octane (NPOE) and tetrahydrofuran (THF) were purchased from Sigma-Aldrich. 2-[4-(2-hydroxyethyl)piperazin-1-yl]ethanesulfonic acid (HEPES buffer) and L-histidine were purchased from TCI Chemicals. All other reagents were of the highest commercially available purity and were used as received. Aqueous solutions of salt and buffer were prepared with ultrapure water (18.2 MΩ) obtained from a PURELAB Option-Q water system. All solutions were prepared as 1M stock and used for serial dilution to prepare working standards; 1M HEPES buffer was prepared and used as-is without further pH adjustments. Carbon (C110) screen-printed electrodes (SPEs) were purchased from Metrohm Dropsens and were used as received.

Preparation of Cl^- SC-ISE. Commercially sourced PEDOT-PEG:ClO_4 dispersion was subjected to 30 min of agitation prior to use. 3 µL of PEDOT-PEG:ClO_4 was drop-casted onto the working electrode of C110 SPEs and dried at 60 °C for 30 min. The PEDOT-PEG:ClO_4 -coated SPEs were immersed in 0.1 M solutions of potassium chloride (K*Cl*) for 3 days for ion exchange. Thereafter, the SPEs were removed, rinsed with DI water and dried under vacuum overnight. ISM cocktail was prepared by dissolving chloride ionophore IV (1.0 mg), TDMA*Cl* (0.5 mg), PVC (32.9 mg), and NPOE (65.9 mg) in THF (1 mL) for the optimal composition (**C1**). 10 µL of ISM was drop-casted onto the chloride-doped PEDOT-PEG SPEs and dried overnight at ambient temperature, followed by drying under vacuum for 4 h. The SC-ISEs were then conditioned in 1 mM K*Cl* solution overnight prior to use. In the case of non-conditioned use (**C5**), SC-ISEs were used as-is after drying with the omission of the overnight conditioning.

X-ray Photoelectron Spectroscopy (XPS). XPS analysis was performed using a Thermo Scientific Theta Probe XPS system with monochromatic Al Kα X-ray source (hv = 1486.7 eV) at 400 µm spot size. Photoelectrons were collected at a take-off angle of 50° with respect to surface normal. Wide scan spectra were acquired with pass energy of 200 eV and step size of 1 eV. Fine scans of C 1s, N 1s, S 2p and Cl 2p were acquired with pass energy of 40 eV at 0.1 eV step size. Combined electron/ion flooding was used for charge

compensation and further charge shift correction was done based on the C-C peak of C 1s at 284.8 eV. **Raman spectroscopy.** Raman spectroscopy was performed using Renishaw inVia confocal Raman microscope with laser wavelength 532 nm at 50x magnification and 2400 g/mm grating. The spectra were acquired at 10 s acquisition time for 1 accumulation.

Cyclic voltammetry (CV). Measurements were performed at room temperature using a Dropsens Potentiostat (DRP-STAT8000, Metrohm Dropsens) in a 3-electrode setup having Ag|AgCl|3M KCl|1M LiOAc as the reference electrode, and platinum sheet as the counter electrode. All potentiometric measurements were performed in triplicate. The cyclic voltammagrams of PEDOT-PEG solid contacts were measured between −1.0 V and +1.0 V, scan rate v = 0.05 V s^{-1}, in 0.1 M K*Cl* solution.

Open circuit potentiometry. Measurements were performed at room temperature using a Dropsens Potentiostat (DRP-STAT8000, Metrohm Dropsens) in a 2-electrode setup with a Ag|AgCl|3M KCl|1M LiOAc reference electrode. Three replicates of each SC-ISE were tested. The sensitivity and limit of detection of the electrode were evaluated by measuring the open circuit potential in KCl solutions with concentration ranging from 1 nM to 0.1 M. Selectivity coefficients were evaluated using the fixed interference method (FIM).[31–33] See ESI for more details. **Current reversal chronopotentiometry.** Chronopotentiometry was performed using a 3-electrode setup in 1 mM aqueous KCl. A current (± 10 nA) was applied to the working electrode, first positive current for 60 s, followed by negative current for 60 s, while the electrode potential was continuously recorded. **Electrochemical Impedance Spectroscopy (EIS).** EIS measurements were performed at room temperature using an Autolab Potentiostat (PGSTAT30, Metrohm Autolab). Nyquist plots were collected in the frequency range of 100 kHz to 1 mHz with a sinusoidal voltage signal of 100 mV. A 3-electrode setup in 1 mM aqueous KCl was used. All impedance spectra were fitted to equivalent circuits using the EIS Spectrum Analyser.

***Cl*⁻ Quantitation in synthetic samples**. Artificial sweat was prepared following ISO-3160-2-2015, artificial urine was prepared following formulation reported by Khan et al.[34] and artificial blood serum was prepared following ISO-10993-15-2000. **Real sweat sample testing.** Real human sweat (forearm samples) was collected from healthy volunteers using 3M Tegaderm +Pad and extracted from the dressing film through a syringe. Four pieces of Tegaderm +Pad were attached onto the forearm of volunteers who then exercised for 1-hour. Only sweat which was collected in the dressing films was sampled to avoid any potential contamination (e.g. from clothing etc.). Subsequently, sweat samples collected were diluted 10 or 100 times with 0.1 M HEPES buffer (pH 6.8). In the case of quantitative analysis of buffered samples, the SC-ISEs were calibrated using buffered K*Cl* solution between the range of 0.1 M to 1 mM. Anionic concentrations were used instead of activities as it is difficult to estimate activity coefficients in zwitterionic buffers.

RESULTS

Characterisation of *Cl*⁻-doped PEDOT-PEG solid-contact. To begin the investigation, PEDOT-PEG solid-contact was first prepared using commercially sourced PEDOT-PEG:*Cl*O_4 dispersion with *Cl*O_4^- anionic dopant. Various studies have shown that the doping species and level in PEDOT solid-contact can affect the properties of the fabricated solid-contact[35–37] as well as SC-ISE performance.[38,39] We have also shown previously in our work on potentiometric ISE that re-doping PEDOT-PEG:*Cl*O_4 solid-contact with the primary analyte enhanced the performance of a NO_3^- SC-ISE.[22] To this end, screen-printed electrode with PEDOT-PEG solid-contact was immersed in 0.1 M K*Cl* for three days to prepare *Cl*⁻-doped PEDOT-PEG solid-contact (PEDOT-PEG:*Cl*) for subsequent fabrication of *Cl*⁻ SC-ISE. OCP monitoring was performed over 77 h to monitor the anion exchange process; stabilisation of the potential was observed between 60-77 h (Figure S1), indicating that ion exchange was completed. Water contact angle measurements (WCA) of 52.3° ± 1.9° and 48.6° ± 1.5° respectively indicate that the solid-contacts also have similar lipophilicities (Figure S2). Although these WCA values are small compared to some of the hydrophobic PEDOT-based solid-contacts reported,[38,40,41] Lindner and co-workers had previously established that they are still sufficient for use as a stable solid-contact.[42] Additionally, scanning electron microscopy showed that the

morphology of the anion-exchanged PEDOT-PEG:*Cl* was structurally similar to its PEDOT-PEG:*Cl*O_4 precursor (Figure S3). Overall, these experiments suggest that no significant structural changes had occurred during anion exchange.

To better understand the performance of our SC-ISEs, a combined analysis of XPS, Raman spectroscopy and CV was performed to characterize the dopant level in the PEDOT-PEG solid-contacts. Using XPS, it was possible to validate the dopant species and level in the PEDOT-PEG solid-contact after the ion exchange process. The XPS wide scan (Figure S4a) indicated the presence of C, O, *Cl*, and S elements, which is expected of Cl^--doped PEDOT-PEG solid-contact. From the *Cl* 2p fine scan (Figure 1a), the disappearance of the characteristic doublet at *ca*. 207.5 eV ($2p_{3/2}$) and 209 eV ($2p_{1/2}$) ascribed to the original ClO_4^- dopant and the appearance of new characteristic doublet at *ca*. 196.7 eV ($2p_{3/2}$) and 198 eV ($2p_{1/2}$) ascribed to new Cl^- dopant is indicative of the successful preparation of PEDOT-PEG:*Cl*. Furthermore, a comparison of the S 2p fine scan (Figure S4b) of the PEDOT-PEG:*Cl*O_4 and the PEDOT-PEG:*Cl* showed that the ion exchange protocol did not alter the structure of the thiophene rings within the PEDOT chain in the solid-contact.

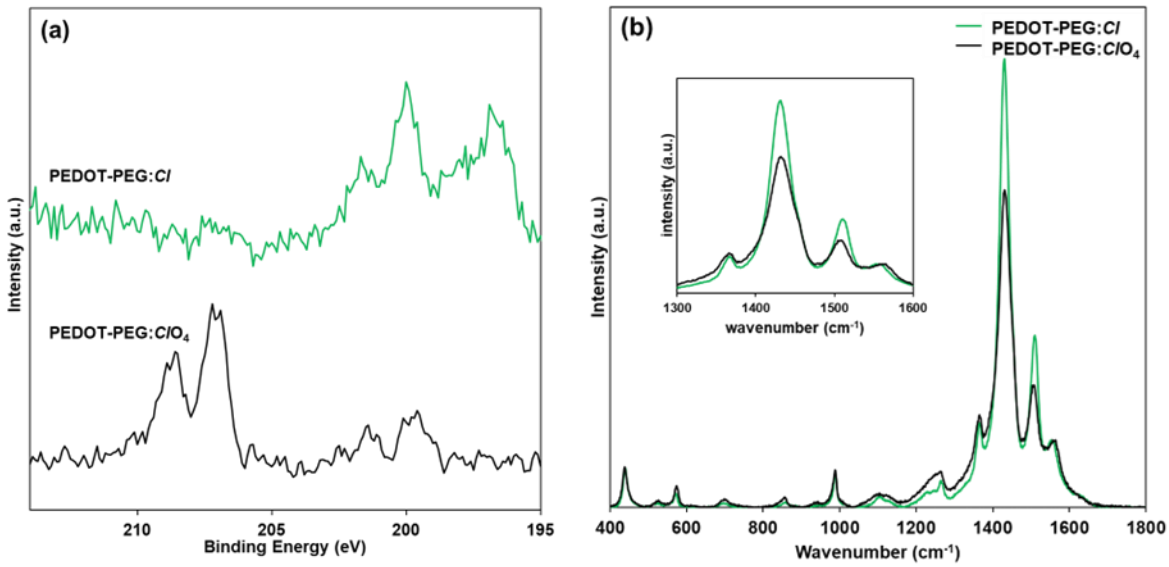

Figure 1. (a) XPS *Cl* 2p fine scan of PEDOT-PEG solid-contacts; (b) normalized Raman spectra (532 nm) of PEDOT-PEG solid-contacts.

Raman spectroscopy was performed to differentiate the doping levels in PEDOT-PEG:*Cl* and PEDOT-PEG:*Cl*O_4 (Figure 1b). The thiophene moieties in the PEDOT chains exist as a mixture of undoped benzoid (semi-conductive) and doped quinoid (conductive) forms with different electronic states.[43–45] Undoped polythiophene exhibits a stronger absorption band at lower wavelength compared to its doped counterpart, which enhances its Raman peak corresponding to the quinoid resonant form when excited by a 532 nm laser beam.[45] Since the structure and the number of oxyethylene rings of PEDOT is not affected by dopant species and doping levels, the Raman spectra can be normalized to the peak at 990 cm^{-1} which corresponds to the oxyethylene ring deformation. This allows a simple comparison of the spectra around the strongest absorption band (*ca*. 1300 – 1500 cm^{-1}) which corresponds to the symmetric C_α=C_β stretching mode of the PEDOT thiophene ring.[43–48] An increase in the intensity of the peaks at 1368 and 1437 cm^{-1} indicated that the undoped benzoid form is the dominant species in PEDOT-PEG:*Cl* as compared to the PEDOT-PEG:*Cl*O_4. Hence, the Raman results suggest that the dopant level in the Cl^--doped PEDOT-PEG solid-contact is lower compared to its ClO_4^--doped counterpart, which is expected as ClO_4^- is a strong dopant.[36] These results are also in alignment with the XPS estimates of dopant concentrations which indicate that the ClO_4^- dopant was present in higher atomic percentage in the PEDOT-PEG:*Cl*O_4 solid-contact as compared with Cl^- anion in its corresponding PEDOT-PEG solid-contact (Table S1). CV experiments (Figures S5-S6) also demonstrated that PEDOT-PEG:*Cl* had a lower oxidation potential and higher

capacitance than PEDOT-PEG:ClO_4, indicating that the former is less doped and hence more easily oxidised.[49]

Potentiometric measurements of Cl^- SC-ISEs. Having evidenced that the ion exchange was successfully performed, Cl^- ISM was drop-casted to fabricate Cl^- SC-ISE **C1** (Table 1). Open-circuit potential measurements were performed in unbuffered K*Cl* solutions between 0.1 M to 1 nM to evaluate the sensitivity of SC-ISE **C1** towards the Cl^- anion (Figure 2a**,** Table 1). Selectivity coefficients for dihydrogen phosphate ($H_2PO_4^-$), hydrogen carbonate (HCO_3^-), acetate (CH_3COO^-), NO_3^- and bromide (Br^-) ion were determined using the fixed interference method (FIM) to mimic actual samples containing both primary and interfering ions.[32,33,50] **C1** exhibited a near-Nernstian response (−53.3 ± 0.5 mV/decade) towards the Cl^- anion with selectivity performances comparable to previously reported work (Figure 2d, Table S2).[51]

Table 1. Sensitivity and detection limit (LOD) of Cl^- SC-ISEs investigated (n = 3)

SC-ISE	Ionophore wt%	PEDOT-PEG dopant	sensitivity/ mV dec^{-1}	LOD / log10(a_{Cl}/ M)
C1[a]	1	Cl^-	−53.3 ± 0.5	−5.22 ± 0.05
C2[a]	3	Cl^-	−51.7 ± 2.2	−5.01± 0.08
C3[a]	5	Cl^-	−51.4 ± 1.6	−4.95 ± 0.07
C4[a]	1	ClO_4^-	−33.4 ± 1.8	−4.46 ± 0.28
C5[b]	1	Cl^-	−51.4 ± 0.9	−5.06 ± 0.11

[a] SC-ISEs were conditioned for 16 h in 1 mM KCl prior to use; [b] SC-ISEs were not conditioned prior to use.

Further studies were conducted to optimize the membrane composition for Cl^- selectivity against more chaotropic ions (NO_3^- and Br^-). Studies by Meier et al. and Eugster et al. have established, theoretically and experimentally, that for monovalent anion with 1:1 binding stoichiometry, 50 mol% of anion exchanger with respect to the amount of ionophore is the ideal composition.[52,53] Hence, for the bis-thiourea ionophore used in this study, the focus was placed on optimizing the weight percentage (wt%) of ionophore used in the Cl^- SC-ISE. The potentiometric response towards Cl^- and potential anionic interferences were evaluated for SC-ISEs containing 1, 3 or 5 wt% ionophore in the ISM with 50 mol% TDMA*Cl* as anionic exchanger (Table 1, Figure S7). Our results indicate that higher wt% ionophore resulted in slight deterioration of both sensitivity slope and limit of detection; the chloride SC-ISE with higher wt% ionophore also suffered from hysteresis. Furthermore, while the results suggest that increasing the wt% of ionophore could potentially lead to an improvement in selectivity for more chaotropic anions (NO_3^- and Br^-), the overall deterioration of selectivity for more kosmotropic anions ($H_2PO_4^-$, HCO_3^- and $CH_3CO_2^-$) rendered the marginal improvement insignificant (Figure 2d, Table S2). Thus, **C1** with 1 wt% of ionophore was determined to be the optimal SC-ISE with good reproducibility between replicates (Figure S8) and the following selectivity coefficients log(*K*) were obtained by FIM: −3.78 for $H_2PO_4^-$; −1.55 for HCO_3^-; −1.98 for CH_3COO^-; +0.52 for NO_3^- and +0.59 for Br^-.

As a control to demonstrate the performance enhancement from the ion exchange protocol, **C4** was prepared by drop-casting the optimal ISM formulation containing 1 wt% ionophore with 50 mol% TDMA*Cl* onto the original PEDOT-PEG:ClO_4 solid-contact without ion exchange and similarly tested for its sensitivity and selectivity performance (Figure 2b). To our surprise, **C4** exhibited poor sub-Nernstian slope (−33.4 ± 1.8 mV/decade) which was not observed previously for the NO_3^- SC-ISE.[22] To further confirm the impact of anion exchange on SC-ISE performance, Cl^- SC-ISE **CV1** was fabricated from the solid-contacts which had undergone electrochemical anion exchange via successive CV cycles in K*Cl*. **CV1** also exhibited improved sensitivity (−48.8 ± 2.4 mV/decade, Figure S9) towards K*Cl*, confirming that the exchange of dopant, regardless of the method, was responsible for improved performance. Additionally, a coated wire electrode (CWE *Cl*), in which ISM was coated directly onto the carbon electrode, exhibited near-Nernstian sensitivity

(−52.3 ± 0.2 mV/decade, Figure S10), suggesting that the original PEDOT-PEG:ClO_4 solid-contact was incompatible in a Cl^- ISE.

Unexpectedly, the selectivity of SC-ISE **C4** appeared to be similar to **C1** (Figure 2d, Table S2), with the exception of $H_2PO_4^-$ selectivity, which could not be accurately determined due to the sub-Nernstian slope. The difference in $H_2PO_4^-$ selectivity could be observed in the aqueous layer test [33,54] performed for **C1** and **C4** (Figure S12). Both SC-ISEs did not exhibit any aqueous layer, with ≤ 3 mV hysteresis in EMF upon returning to the 0.1 M KCl solution despite the relatively small WCA.[42] However, a much larger potential change was observed for **C1** when the solution was changed from 0.1 M K*Cl* (primary ion) to 0.1 M KH_2PO_4 (interfering ion) and back, corroborating the superior selectivity performance of **C1**. Additionally, **C1** exhibited less long-term potential drift compared to **C4**.

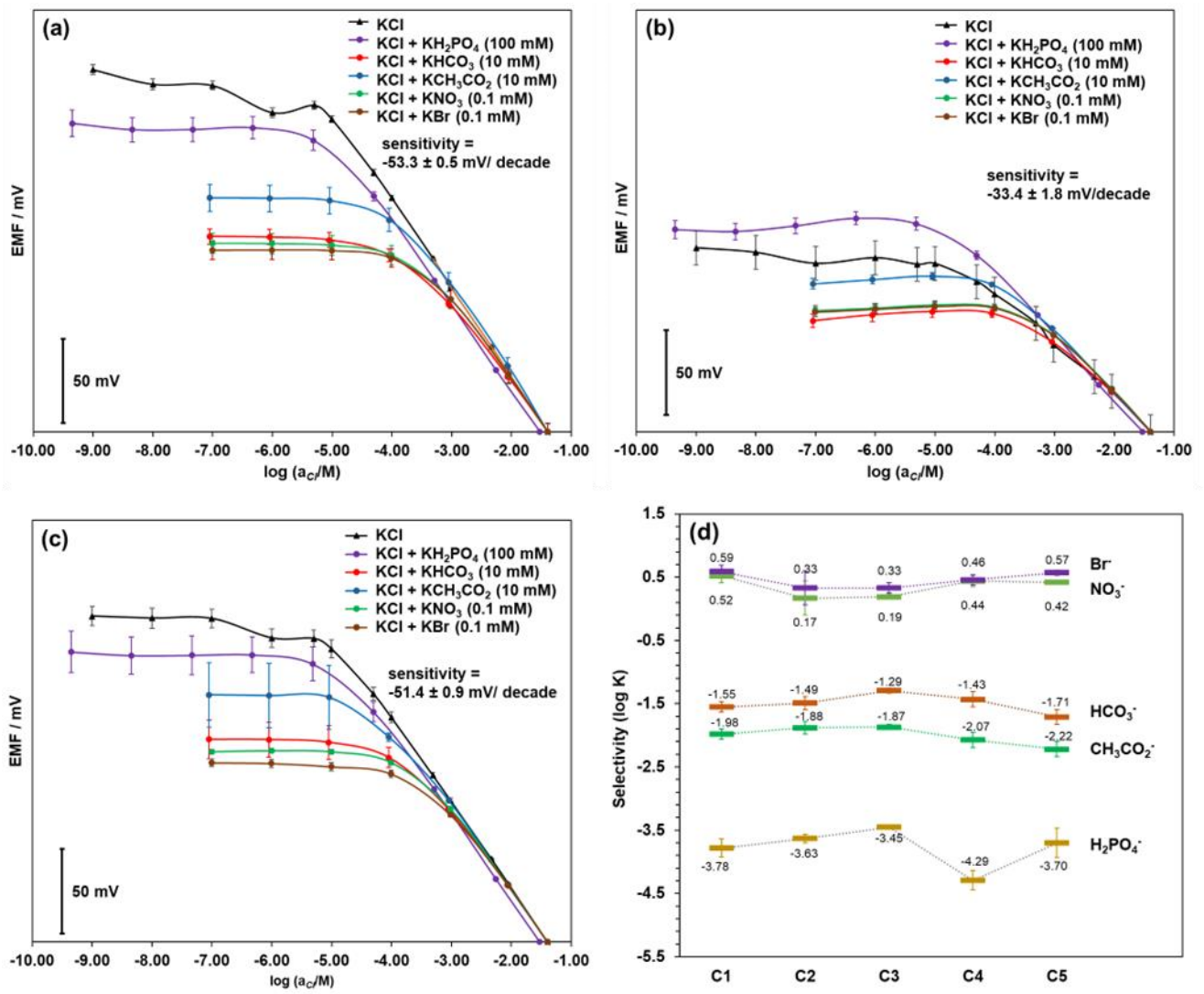

Figure 2. Potentiometric response of (a) **C1**; (b) **C4**; (c) **C5** toward Cl^- anion in pure (black) and mixed solutions containing fixed amounts of interfering ions; and (d) comparison of the potentiometric selectivity coefficients ($\log_{10}K$) of Cl^- SC-ISE **C1** to **C5** against various interfering ions determined by FIM.

Table 2. Potentiometric response of C1 after soaking in 0.1 M KCl for 28 days. (n = 2)

	Day 0	Day 1	Day 4	Day 7	Day 11	Day 15	Day 21	Day 28
Sensitivity/ mV dec^{-1}	53.2 ± 1.9	52.4 ± 0.8	51.8 ± 0.4	51.6 ± 0.0	51.2 ± 0.1	50.3 ± 0.6	48.2 ± 0.1	44.2 ± 0.0

This difference in potential drift was also observable in the short-term using current reversal chronopotentiometry (Figure S14, Table S3).[20,55] The short-term potential drift was determined after the current polarity change and used to estimate the low-frequency capacitance (C_{LF}) of **C1** and **C4** via the equation $E/t = i/C_{LF}$. The results show that **C1** exhibited lower drift (196.1 μV s^{-1}), thus higher capacitance (51 μF) as compared to **C4.** This indicates that PEDOT-PEG:*Cl* dopant is a more stable ion-to-electron transducer.

Additionally, lifespan testing was performed by continuous immersion of **C1** in 0.1 M K*Cl* for a period of 28 days to simulate continuous usage (Table 2, Figure S13). All Cl^- SC-ISEs were kept dry for a minimum of 8 days before OCP measurement. **C1** was able to retain its sensitivity within ±5 mV/decade (48.2 ± 0.1 mv/decade) after a period of 21 days in 0.1 M K*Cl*, indicating good stability for prolonged usage within this period. When tested on Day 28, significant deterioration of the sensitivity performance of **C1**'s performance was observed, indicating that it should not be used continuously for more than 21 days.

Circumventing conditioning time of Cl^- SC-ISE. Most ISEs require a conditioning step before each use.[56] During conditioning, the ISM is allowed to pre-equilibrate in a solution of the primary ion via ionophore-ion complexation. This process is crucial to achieve a constant primary ion activity within the ISM so that transmembrane ion fluxes are minimised and a Nernstian response could be obtained. Conditioning protocols can take between 12 to 72 hours, rendering most existing ISEs impossible to be used instantaneously. Hence, a readily usable SC-ISE is of great relevance and interest today.[57,58]

Rich et al. and Armas et al. have previously shown that by pre-loading the ISM formulation with the primary ion, the traditional requirement for ISE conditioning can be circumvented.[57,59] Since our optimal SC-ISE **C1** contains the Cl^- anion in both the ISM and the PEDOT-PEG solid-contact, we hypothesized that it could also be used similarly. To this end, SC-ISE **C5** (with same composition as **C1**) was fabricated and evaluated without prior conditioning before use. Gratifying, **C5** performed well with comparable selectivity to **C1**, albeit with slightly deteriorated slope (Figure 2c, Table 1). This omission of the lengthy conditioning protocol allows a significant reduction in the operational ready time of the SC-ISE and simplifies its operation.

Electrochemical Investigation of Cl^- SC-ISEs. To investigate the origin of the difference in sensitivity performances, EIS was performed on CWE *Cl* and SC-ISEs **C4** and **C1** (Figures 3a-c respectively). Unlike current reversal chronopotentiometry, the frequency sweep offered by EIS enabled us to fully characterize the impedance response of the electrodes. For all Nyquist plots, the high frequency semicircle is attributed to the bulk resistance of membrane (R1). This was reasonably concluded from a series of experiments where the thickness of the membrane layer was modified.

Both CWE *Cl* and **C1** exhibited a depressed semicircle (R1CPE1) with a smaller n value (Table S4) compared to **C4**, indicating non-ideal capacitance, albeit with larger magnitude of the constant phase element (CPE).[60] This suggests good overlap between the ISM and transduction layer – either the carbon electrode for CWE *Cl* or the PEDOT-PEG:*Cl* solid-contact for **C1**.[14,61] At lower frequency, the Nyquist plot for **C1** only features a 45° line (fitted as CPE2 with n = 0.46), indicating that PEDOT-PEG:*Cl* is an effective ion-to-electron transducer with minimal charge transfer resistance at the interface. In contrast, a semicircle was observed for both CWE *Cl* and **C4**, with charge transfer resistance (R2) of *ca*. 110 kΩ for CWE *Cl* and even larger at *ca*. 1268 kΩ for **C4**. This indicates blocked transduction when PEDOT-PEG:ClO_4 is used as a solid-contact in **C4**, resulting in poor sensitivity of the SC-ISE (Figure 2b).[62–64] This finding was unexpected as it contradicts our previous work,[22] in which the NO_3^- SC-ISE with PEDOT-PEG:ClO_4 solid-contact exhibited low charge transfer resistance and good sensitivity, but poor selectivity (Figures S15-S16).

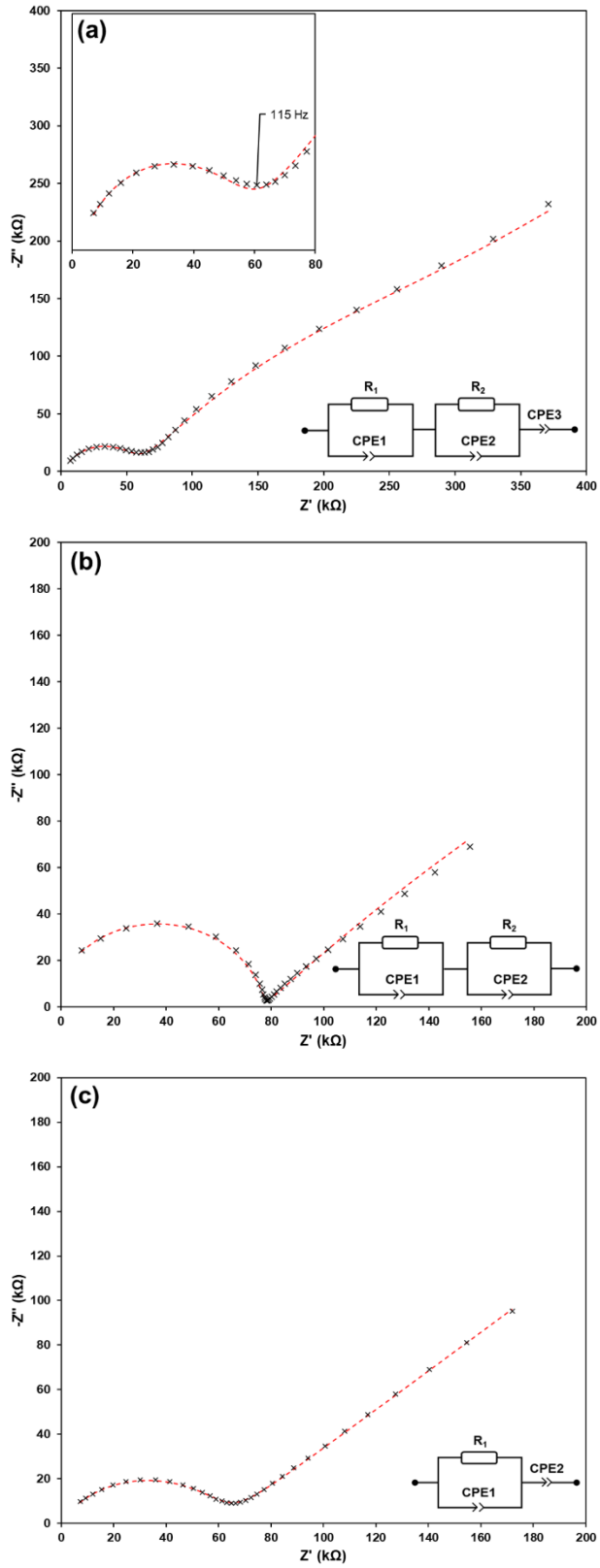

Figure 3. Nyquist plots and fitted impedance spectrum of (a) CWE *Cl* and chloride SC-ISEs (b) **C4** with ClO_4^- dopant and (c) **C1** with Cl^- dopant. The inset in (a) shows high-frequency semicircle (*ca.* 10 kHz −115 Hz) of CWE *Cl*. The equivalent circuits used for fitting impedance data are shown in each spectrum. Frequency range: 100 kHz to 0.1 Hz; amplitude potential: 100 mV; solution: 1 mM K*Cl*.

Anion dopant exchange: Does it affect sensitivity or selectivity? We hypothesised that the differences between the Cl^- and NO_3^- SC-ISEs may be attributed to the addition of ionophore in the ISM in this work, which restricts movement of the ClO_4^- anions out of the solid-contact. Indeed, XPS confirmed that no ClO_4^- anion was present in the *Cl* 2p fine scan of the ISM surface of **C1** and **C4**. In contrast, the characteristic doublet ascribed to ClO_4^- at *ca*. 207.5 eV ($2p_{3/2}$) and 209 eV ($2p_{1/2}$) was present in the ISM surface of the NO_3^- SC-ISE we previously reported with PEDOT-PEG:ClO_4 solid-contact (Figure S17).[22] In addition, while Raman analysis demonstrated that the bare PEDOT-PEG:ClO_4 solid-contact was more heavily doped than its anion-exchanged PEDOT-PEG:*Cl* counterpart (Figure 1b), analysis of the PEDOT-PEG layer in the SC-ISEs showed that the NO_3^- SC-ISE with PEDOT-PEG:ClO_4 solid-contact exhibited lower doping levels similar to **C1** instead of the high doping levels still observed in **C4** (Figure S18). Together, these findings suggest that the excess ClO_4^- anions could migrate from the PEDOT-PEG layer into the ISM when only lipophilic salt was present, while the presence of ionophore in **C4** may prevent this migration.

This information can be put together with the potentiometric and EIS data to potentially explain the different mechanisms of performance enhancement via PEDOT-PEG anion exchange. In both **C4** and the NO_3-ISE with the original ClO_4^--doped solid-contact, there initially was a huge excess of ClO_4^- anions in the PEDOT-PEG:ClO_4 layer, which was observed by XPS (Table S1) and Raman spectroscopy (Figure 1b). For **C4**, the presence of chloride ionophore prevents partitioning of ClO_4^- into the ISM (Figure S17), thus the excess ClO_4^- remained immobilised in the solid-contact (Figure S18). This restricts doping of PEDOT-PEG by Cl^- anions in the ISM, leading to blocked transduction (Figure 4a),[62–64] which was observed in the EIS (Figure 3b) as resistance R2. While this is known for anion-selective membranes with PEDOT:poly(styrene sulfonate) (PSS) due to the bulky, immobile PSS anion, this finding is more surprising for molecular anions as they are expected to be mobile.[62,63] In potentiometric measurements, this was manifested as low sensitivity to changes in solution Cl^- concentration (Figure 2b). In contrast, when the dopant and analyte anion are mobile and identical, such as in **C1**, the analyte anion in the ISM can equilibrate with the solution and dope PEDOT-PEG with ease (Figure 4b), enabling good sensitivity and selectivity (Figure 2a).

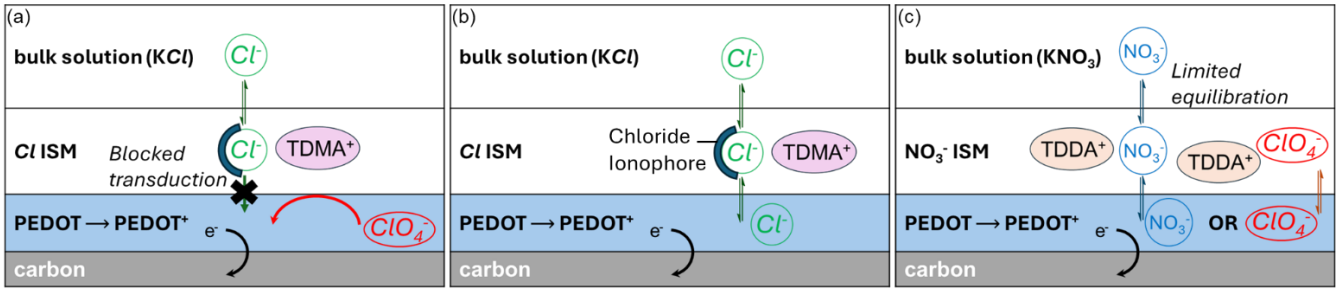

Figure 4. Schematics showing ion movements in anion SC-ISEs with PEDOT-PEG solid-contact for (a) **C4**, (b) **C1** and (c) NO_3^- ISM coated on PEDOT-PEG solid-contact with ClO_4^- dopant. (a) The presence of ionophore in **C4** prevented movement of ClO_4^- into the ISM and hindered the entry of Cl^- into the PEDOT-PEG solid-contact, hence resulting in blocked transduction; (b) Cl^- can equilibrate with solution and dope the solid-contact, thus enabling **C1** to exhibit good sensitivity and selectivity; (c) The absence of ionophore allowed ClO_4^- to migrate into the ISM, NO_3^- can dope the solid-contact but selectivity is poor due to presence of interfering ClO_4^-. The composition of the ISM matrices have been simplified for clarity of presentation; for full composition please refer to experimental section. ISM = ion-selective membrane; PEDOT = poly(3,4-ethylenedioxythiophene), TDMA = tridodecylmethylammonium, TDDA = tetradodecylammonium.

In the NO_3^- SC-ISE with the original ClO_4^--doped solid-contact, the absence of ionophore enabled excess ClO_4^- anions to migrate into the ISM (Figure S17) and lowered the doping level of PEDOT-PEG (Figure S18). This allows doping of PEDOT-PEG by either NO_3^- or ClO_4^- anions, thus no impediment to sensitivity was observed (Figure 4c). However, equilibration of NO_3^- with the solution is limited due to presence of ClO_4^- anions in the ISM (Figure S17) coordinating to the cationic lipophilic additive. This diffusion-limiting

resistance (R3) was observed in the EIS (Figure S16) and in potentiometric measurements was manifested as poor selectivity (Figure S15).[22] Thus, when NO_3^- replaced ClO_4^- as anionic dopant in the PEDOT-PEG solid-contact, selectivity was significantly improved.

Although our findings appeared contradictory at first glance, the combination of analytical techniques enabled a deeper understanding of the different mechanisms of performance enhancement. This can be applied broadly to the development of anion-selective SC-ISEs utilising conducting polymers as solid-contacts.

Determination of *Cl*⁻ in Samples of Biological Relevance. The foremost important evaluation of every newly developed sensor is its applicability to real sample analysis.[65] Chloride determination is of great clinical significance as it is an important biomarker that is used to diagnose a variety of medical diseases.[1–7] Particularly, cystic fibrosis (CF) is a genetic disorder that affects the ability of the body to regulate movement of water and salt in and out of cells, consequently resulting in accumulation of thick mucus within the body's tubes and passageways that can cause recurrent infections. When left untreated, cystic fibrosis would result in severe damage to the lungs along with other organs in the body. Currently, CF is diagnosed by a sweat test, in which sweat is collected and sent to a laboratory for determination of chloride levels.[1–3] Clinically, chloride quantification is conducted using techniques such as anion chromatography or coulometric titration. [66] While these methods are highly accurate and precise, they typically have a large footprint and require sample pretreatment or chemical derivatization which make them unsuitable for on-site testing. Hence, an alternative analytical method that is rapid, simple, and cost- effective is highly desirable. To this end, the feasibility of the SC-ISE **C1** for the determination of chloride concentration in physiological samples were investigated using artificially prepared human samples (sweat, urine and blood serum) and real human sweat.

As pH varies across physiological samples, a pH test was first performed to determine the pH sensitivity of **C1** (Figure S11). The operational pH range, in which the potential change of **C1** did not exceed ±5 mV, was *ca*. 4 – 7.5. Due to the limited operational pH range, it was necessary to buffer the physiological samples to ensure accurate quantification; 0.1 M HEPES buffer was thus chosen as previously reported by Xiao et al.[51] For consistency, a 1 M stock solution of HEPES buffer (pH 6.8) was prepared and used as-is to perform a 10-times dilution for all artificial physiological samples. To verify the accuracy of chloride quantification, samples with higher chloride concentration (urine and blood serum) were also prepared in 100-times dilution.

Table 3. Quantification performance of *Cl*⁻ SC-ISE **C1**

Sample	Expected stock concentration / mM	Measured stock concentration / mM
synthetic samples		
sweat 10x diluted[a]	85.8	86.1 ± 0.4
urine 10x diluted[b]	139.9	130.6 ± 0.8
urine 100x diluted[b]		140.1 ± 2.1
blood 10x diluted[c]	125.6	119.8 ± 1.1
blood 100x diluted[c]		129.0 ± 2.6
real sample		
sweat 10x diluted	67.1[d]	73.0 ± 1.3

[a] artificial sweat prepared following ISO-3160-2-2015; [b] artificial urine prepared following formulation report by Khan et al.[34]; [c] artificial blood serum prepared following ISO-10993-15-2000; [d] determined through anion chromatography.

The determination of chloride concentrations was performed in triplicate using three separate **C1** SC-ISEs. For each replicate, a standard calibration was performed using HEPES-buffered solutions of K*Cl*

(concentration range between 0.1 M to 0.5 mM) before immersion into HEPES-buffered samples. Our results showed that **C1** was able to determine the chloride concentration of the HEPES-buffered synthetic physiological samples in good agreement with the expected value with less than ± 2% deviation on the logarithmic scale (Table 3).

To further demonstrate the real-world applicability of our sensors, real human sweat (forearm samples) was collected from healthy volunteers using 3M Tegaderm +Pad and similarly tested (Figure S19). Our sensor measurements were in good agreement with the expected value obtained from anion chromatography with less than ± 3.1 % deviation on the logarithmic scale (Table 3).

CONCLUSION

In summary, we have developed a solution-printable chloride-selective SC-ISE via a simple ion exchange protocol. Sensitivity of the SC-ISE was significantly improved by anion exchange, as evidenced by XPS and potentiometric measurements. The best-performing SC-ISE, **C1**, exhibited near-Nernstian response (−53.3 ± 0.5 mV/decade) with a wide dynamic range (0.05 M to 6.03 μM) and long-term potential stability as shown by the aqueous layer test. EIS studies showed that the anion exchange step was necessary to eliminate the blocked transduction arising from the excess ClO_4^- ions in the original PEDOT-PEG solid-contact, which led to a significant decrease in charge transfer resistance and thus improved chloride sensitivity. We further demonstrated that the same anion exchange step could enhance the performance of anion SC-ISEs via different mechanisms – sensitivity or selectivity – depending on whether an ionophore was present in the ISM, increasing the scope and versatility of our protocol.[22,30]

Table 4. Comparison of reported Cl^- SC-ISEs

Solid-contact [a]	Synthesis of solid-contact	Ionophore [c]	Lipophilic Salt	Sensitivity	LOD [e]	$\log_{10} K_{Cl,HCO3}$	$\log_{10} K_{Cl,NO3}$	$\log_{10} K_{Cl,Br}$	Ref
PEDOT:*Cl* [b]	Electrochemical polymerization [b]	-	-	−57.9 ± 0.1	$10^{-3.9}$	+1.7 ± 0.2	+1.0 ± 0.1	+1.1 ± 0.1	[23] [g]
PEDOT:*Cl*	Electrochemical polymerization	-	TDMA-*Cl*	−62.7 ± 0.1	$10^{-3.9}$	−1.2 ± 0.6	+2.0 ± 0.1	+1.6 ± 0.1	[23] [g]
PPy:*Cl*	Electrochemical polymerisation	-	MTAA-*Cl* [d]	−48.4 ± 0.7	$10^{-4.7}$	N.D. [f]	N.D. [f]	N.D. [f]	[24] [g]
POT	Drop-cast	-	TDMA-*Cl*	−46.9 ± 1.1	$10^{-5.0}$	-1.6 ± 0.4	+2.1 ± 0.0	+1.4 ± 0.1	[25] [g]
PANINFs:*Cl* MWCNT	Interfacial polymerization + drop-cast	Chloride ionophore III	TDMA-*Cl*	−61.3± 1.5	N.D. [f]	−4.8	−4.6	−1.6	[26] [g]
Nanowire PEDOT:*Cl*	Electrochemical polymerization	Chloride ionophore III	TDMA-*Cl*	−58.1	$10^{-5.0}$	−4.5	−0.8	+0.8	[27] [g]
PAAm-MnO_2	Electrochemical deposition	Chloride ionophore IV	TDMA-*Cl*	−52.2	$10^{-5.0}$	−1.9	−0.1	+0.2	[28] [h]
Liquid-filled ISE	N.A.	Chloride ionophore IV	TDMA-*Cl*	−54.0 ± 1.0	$10^{-5.2}$	−2.6 [i]	+0.7 [j]	+0.4 [j]	[51]
PEDOT-PEG:*Cl*	Drop-cast with ion exchange	Chloride ionophore IV	TDMA-*Cl*	−53.3 ± 0.5	$10^{-5.2}$	−1.6 ± 0.1	+0.5 ± 0.1	+0.6 ± 0.1	this work [h]

[a] PEDOT = poly(3,4-ethylenedioxythiophene); PANINFs-*Cl* = chloride-doped polyaniline nanofibers; MWCNT = multiwalled carbon nanotubes; PAAm = poly(allylamine); PPy-*Cl* = chloride-doped poly(pyrrole) films, POT = poly(3-octylthiophene); [b] PEDOT:*Cl* was used directly as the sensing membrane; [c] Chloride ionophore III = 3,6-didodecyloxy-4,5-dimethyl-*o*-phenylene-bis(mercury chloride), Chloride ionophore IV = 4,5-bis-[*N*-(butyl)thioureido]-2,7-di-*tert*-butyl-9,9-dimethylxanthene; [d] MMTA-*Cl* = methyl tri-*n*-tetradecylammonium chlo-

ride; [e] LOD = limit of detection; [f] N.D. = not determined. Selectivity coefficients were determined using [g] SSM, [h] FIM, or the matched potential method (MPM) for chloride concentration from [i] $10^{-5.0}$ to $10^{-4.7}$, or [j] $10^{-2.34}$ to $10^{-2.04}$.

In comparison to other recently reported chloride-selective SC-ISEs (Table 4), our chloride-selective SC-ISEs demonstrated better detection range and comparable sensitivity. While the selectivity of our chloride SC-ISE seems modest, it is comparable to other ISEs using the same ionophore (Chloride ionophore IV),[28] which is safer than the mercury-containing Chloride ionophore III, which can be toxic to both the user and the environment.[23,26,27] Additionally, the selectivity of our SC-ISEs were tested via FIM, which is more indicative of real samples than the more commonly used separate solution method (SSM). Noteworthy, potentiometric studies demonstrated that our chloride-selective SC-ISE could be used with a short conditioning period prior to measurement, enhancing ISM pretreatment efficiency. Lifespan studies also demonstrated that our chloride-selective SC-ISE could maintain its sensitivity within ±5 mv/decade (48.2 ± 0.1 mV/decade) under prolonged usage of up to 21 days.

Finally, we demonstrated the applicability of our chloride-selective SC-ISE in health monitoring by determining chloride concentration in real human sweat samples with good reproducibility and accuracy. Furthermore, we also demonstrated the potential applications to other types of biological samples through accurate chloride quantification in synthetic urine and blood samples. Apart from solution-processability, our chloride-selective SC-ISE also offers improved sensitivity and fabrication efficiency, which will greatly benefit its utilization for on-site applications such as environmental, food safety and healthcare monitoring.

SUPPORTING INFORMATION

The Supporting Information is available free of charge.

ACKNOWLEDGMENT

The authors would like to thank Dr Debbie HL Seng for her assistance in X-ray photoelectron spectroscopy experiments, Ms Hnin Yu Yu Ko for her assistance in Raman spectroscopy experiments, Ms Coryl JJ Lee for her assistance in SEM imaging, our healthy volunteer for the real sweat sample and NUS CMMAC for anion chromatography analysis.

AUTHOR CONTRIBUTION

Conceptualization – S.S.G.; Funding – S.S.G.; Investigation – S.H. Ng, G.E.K.K. Seah; Methodology – S.H. Ng, G.E.K.K. Seah, D.S.; Supervison – S.S.G.; Writing – original draft – S. H. Ng, G.E.K.K. Seah; Writing – review and editing – G.E.K.K. Seah, D.S., S.S.G.

FUNDING SOURCES

This work was supported by the Agency of Science, Technology and Research (A*STAR) under its Career Development Fund (CDF) Grant (C210112021) and Manufacturing, Trade And Connectivity (MTC) Programmatic Fund (M22K9b0049).

DECLARATION

S.S. Goh, G.E.K.K. Seah and S.H. Ng are listed as inventors on a patent application based on the results presented herein.

REFERENCES

[1] K. De Boeck, F. Vermeulen, L. Dupont, The diagnosis of cystic fibrosis, Presse Med. 46 (2017) e97–e108. https://doi.org/10.1016/J.LPM.2017.04.010.

[2] A.C. Gonçalves, F.A.L. Marson, R.M.H. Mendonça, C.S. Bertuzzo, I.A. Paschoal, J.D. Ribeiro, A.F. Ribeiro, C.E. Levy, Chloride and sodium ion concentrations in saliva and sweat as a method to diagnose cystic fibrosis, J. Pediatr. (Rio. J). 95 (2019) 443–450. https://doi.org/10.1016/j.jped.2018.04.005.

[3] A.C. Gonçalves, F.A. de L. Marson, R.M. de H. Mendonça, J.D. Ribeiro, A.F. Ribeiro, I.A. Paschoal, C.E. Levy, Saliva as a potential tool for cystic fibrosis diagnosis, Diagn. Pathol. 8 (2013). https://doi.org/10.1186/1746-

1596-8-46.
[4] M. Khatri, J. Zitovsky, D. Lee, K. Nayyar, M. Fazzari, C. Grant, The association between serum chloride levels and chronic kidney disease progression: A cohort study, BMC Nephrol. 21 (2020). https://doi.org/10.1186/s12882-020-01828-3.
[5] A.J.L. Zandijk, M.R. van Norel, F.E.C. Julius, N. Sepehrvand, N. Pannu, F.A. McAlister, A.A. Voors, J.A. Ezekowitz, Chloride in Heart Failure: The Neglected Electrolyte, JACC Hear. Fail. 9 (2021) 904–915. https://doi.org/10.1016/j.jchf.2021.07.006.
[6] Y. Ji, L. Li, Lower serum chloride concentrations are associated with increased risk of mortality in critically ill cirrhotic patients: an analysis of the MIMIC-III database, BMC Gastroenterol. 21 (2021). https://doi.org/10.1186/s12876-021-01797-3.
[7] G. Semmler, B. Scheiner, L. Balcar, R. Paternostro, B. Simbrunner, M. Pinter, M. Trauner, M. Bofill Roig, E.L. Meyer, B.S. Hofer, M. Mandorfer, D.J. Pinato, C. Zauner, T. Reiberger, G.C. Funk, Disturbances in sodium and chloride homeostasis predict outcome in stable and critically ill patients with cirrhosis, Aliment. Pharmacol. Ther. 58 (2023) 71–79. https://doi.org/10.1111/apt.17507.
[8] D.H. Choi, J.S. Kim, G.R. Cutting, P.C. Searson, Wearable potentiometric chloride sweat sensor: The critical role of the salt bridge, Anal. Chem. 88 (2016) 12241–12247. https://doi.org/10.1021/ACS.ANALCHEM.6B03391.
[9] J. Gonzalo-Ruiz, R. Mas, C. de Haro, E. Cabruja, R. Camero, M.A. Alonso-Lomillo, F.J. Muñoz, Early determination of cystic fibrosis by electrochemical chloride quantification in sweat, Biosens. Bioelectron. 24 (2009) 1788–1791. https://doi.org/10.1016/J.BIOS.2008.07.051.
[10] V.A.T. Dam, M.A.G. Zevenbergen, R. van Schaijk, Toward wearable patch for sweat analysis, Sensors Actuators B Chem. 236 (2016) 834–838. https://doi.org/10.1016/J.SNB.2016.01.143.
[11] H.Y.Y. Nyein, M. Bariya, B. Tran, C.H. Ahn, B.J. Brown, W. Ji, N. Davis, A. Javey, A wearable patch for continuous analysis of thermoregulatory sweat at rest, Nat. Commun. 2021 121 12 (2021) 1–13. https://doi.org/10.1038/s41467-021-22109-z.
[12] R. Cánovas, S. Padrell Sánchez, M. Parrilla, M. Cuartero, G.A. Crespo, Cytotoxicity Study of Ionophore-Based Membranes: Toward On-Body and in Vivo Ion Sensing, ACS Sensors 4 (2019) 2524–2535. https://doi.org/10.1021/ACSSENSORS.9B01322.
[13] H. Wu, G. Yang, K. Zhu, S. Liu, W. Guo, Z. Jiang, Z. Li, Materials, Devices, and Systems of On-Skin Electrodes for Electrophysiological Monitoring and Human–Machine Interfaces, Adv. Sci. 8 (2021) 2001938. https://doi.org/10.1002/ADVS.202001938.
[14] J. Hu, A. Stein, P. Bühlmann, Rational design of all-solid-state ion-selective electrodes and reference electrodes, TrAC - Trends Anal. Chem. 76 (2016) 102–114. https://doi.org/10.1016/j.trac.2015.11.004.
[15] Y. Shao, Y. Ying, J. Ping, Recent advances in solid-contact ion-selective electrodes: Functional materials, transduction mechanisms, and development trends, Chem. Soc. Rev. 49 (2020) 4405–4465. https://doi.org/10.1039/c9cs00587k.
[16] H.Y.Y. Nyein, W. Gao, Z. Shahpar, S. Emaminejad, S. Challa, K. Chen, H.M. Fahad, L.C. Tai, H. Ota, R.W. Davis, A. Javey, A Wearable Electrochemical Platform for Noninvasive Simultaneous Monitoring of Ca2+ and pH, ACS Nano 10 (2016) 7216–7224. https://doi.org/10.1021/acsnano.6b04005.
[17] M. Parrilla, M. Cuartero, G.A. Crespo, Wearable potentiometric ion sensors, TrAC - Trends Anal. Chem. 110 (2019) 303–320. https://doi.org/10.1016/j.trac.2018.11.024.
[18] M. Vázquez, P. Danielsson, J. Bobacka, A. Lewenstam, A. Ivaska, Solution-cast films of poly(3,4-ethylenedioxythiophene) as ion-to-electron transducers in all-solid-state ion-selective electrodes, Sensors Actuators, B Chem. 97 (2004) 182–189. https://doi.org/10.1016/j.snb.2003.08.010.
[19] A. Michalska, K. Maksymiuk, All-plastic, disposable, low detection limit ion-selective electrodes, Anal. Chim. Acta 523 (2004) 97–105. https://doi.org/10.1016/J.ACA.2004.07.020.
[20] J. Bobacka, Potential stability of all-solid-state ion-selective electrodes using conducting polymers as ion-to-electron transducers, Anal. Chem. 71 (1999) 4932–4937. https://doi.org/10.1021/ac990497z.
[21] G.E.K.K. Seah, A.Y.X. Tan, Z.H. Neo, J.Y.C. Lim, S.S. Goh, Halogen Bonding Ionophore for Potentiometric Iodide Sensing, Anal. Chem. 93 (2021) 15543–15549. https://doi.org/10.1021/acs.analchem.1c03719.
[22] Z.H. Neo, G.E.K.K. Seah, S.H. Ng, D. Safanama, D.H.L. Seng, S.S. Goh, Solution-Printable PEDOT Solid-Contact for Nitrate-Selective Electrodes: Enhanced Selectivity from Anion Dopant Exchange, Anal. Chem. 94 (2022) 15953–15963. https://doi.org/10.1021/ACS.ANALCHEM.2C02119.
[23] P. Sjöberg-Eerola, J. Bobacka, A. Lewenstam, A. Ivaska, All-solid-state chloride sensors based on electronically conducting, semiconducting and insulating polymer membranes, Sensors Actuators B Chem. 127 (2007) 545–553. https://doi.org/10.1016/J.SNB.2007.05.004.
[24] R. Zielińska, E. Mulik, A. Michalska, S. Achmatowicz, M. Maj-Zurawska, All-solid-state planar miniature ion-selective chloride electrode, Anal. Chim. Acta 451 (2002) 243–249. https://doi.org/10.1016/S0003-

2670(01)01407-6.
[25] P. Sjöberg-Eerola, J. Nylund, J. Bobacka, A. Lewenstam, A. Ivaska, Soluble semiconducting poly(3-octylthiophene) as a solid-contact material in all-solid-state chloride sensors, Sensors Actuators B Chem. 134 (2008) 878–886. https://doi.org/10.1016/J.SNB.2008.06.041.
[26] K. Pietrzak, K. Morawska, S. Malinowski, C. Wardak, Chloride Ion-Selective Electrode with Solid-Contact Based on Polyaniline Nanofibers and Multiwalled Carbon Nanotubes Nanocomposite, Membranes (Basel). 12 (2022) 1150. https://doi.org/10.3390/MEMBRANES12111150.
[27] Z. Li, M. Lei, J. Chen, X. Qi, An All-Solid-State Polymeric Membrane chloride ion-selective Electrode with Nanowires poly(3,4-ethylenedioxythiophene) as Solid Contact, Int. J. Electrochem. Sci. 12 (2017) 11715–11727. https://doi.org/10.20964/2017.12.44.
[28] K. Tsuchiya, T. Akatsuka, Y. Abe, S. Komaba, Design of all-solid-state chloride and nitrate ion-selective electrodes using anion insertion materials of electrodeposited poly(allylamine)-MnO2 composite, Electrochim. Acta 389 (2021) 138749. https://doi.org/10.1016/J.ELECTACTA.2021.138749.
[29] Z.M. Png, K.K.G.E. Seah, M.H. Chua, Q. Zhu, S.S. Goh, J. Xu, Functionalized Poly(azulenes) and Their Electrochromic Properties, ChemistrySelect 8 (2023) e202302183. https://doi.org/10.1002/SLCT.202302183.
[30] S.S. Goh, Z.H. Neo, G.E.K.K. Seah, W.P. Goh, S.H. Ng, Fully Solution-Printed Flexible Solid-Contact Ion-Selective Electrodes, PCT/SG2023/050588, 2023.
[31] Y. Umezawa, K. Umezawa, H. Sato, Selectivity coefficients for ion-selective electrodes: recommended methods for reporting selectivity coefficients values, Pure Appl. Chem. 67 (1995) 507–518.
[32] R.P. Buck, E. Lindner, Recomendations for nomenclature of ion-selective electrodes (IUPAC recommendations 1994), Pure Appl. Chem. 66 (1994) 2527–2536. https://doi.org/10.1351/pac199466122527.
[33] E. Lindner, Y. Umezawa, Performance evaluation criteria for preparation and measurement of macro- and microfabricated ion-selective electrodes (IUPAC Technical Report), Pure Appl. Chem. 80 (2008) 85–104. https://doi.org/10.1351/pac200880010085.
[34] L.B. Khan, H.M. Read, S.R. Ritchie, T. Proft, Artificial Urine for Teaching Urinalysis Concepts and Diagnosis of Urinary Tract Infection in the Medical Microbiology Laboratory, J. Microbiol. Biol. Educ. 18 (2017). https://doi.org/10.1128/jmbe.v18i2.1325.
[35] G. Zotti, S. Zecchin, G. Schiavon, F. Louwet, L. Groenendaal, X. Crispin, W. Osikowicz, W. Salaneck, M. Fahlman, Electrochemical and XPS Studies toward the Role of Monomeric and Polymeric Sulfonate Counterions in the Synthesis, Composition, and Properties of Poly(3,4-ethylenedioxythiophene), Macromolecules 36 (2003) 3337–3344. https://doi.org/10.1021/MA021715K.
[36] S.A. Spanninga, D.C. Martin, Z. Chen, X-ray Photoelectron Spectroscopy Study of Counterion Incorporation in Poly(3,4-ethylenedioxythiophene) (PEDOT) 2: Polyanion Effect, Toluenesulfonate, and Small Anions, J. Phys. Chem. C 114 (2010) 14992–14997. https://doi.org/10.1021/JP104591D.
[37] Z.A. King, C.M. Shaw, S.A. Spanninga, D.C. Martin, Structural, chemical and electrochemical characterization of poly(3,4-Ethylenedioxythiophene) (PEDOT) prepared with various counter-ions and heat treatments, Polymer (Guildf). 52 (2011) 1302–1308. https://doi.org/10.1016/j.polymer.2011.01.042.
[38] S. Papp, M. Bojtár, R.E. Gyurcsányi, T. Lindfors, Potential Reproducibility of Potassium-Selective Electrodes Having Perfluorinated Alkanoate Side Chain Functionalized Poly(3,4-ethylenedioxytiophene) as a Hydrophobic Solid Contact, Anal. Chem. 91 (2019) 9111–9118. https://doi.org/10.1021/acs.analchem.9b01587.
[39] T. Han, U. Mattinen, Z. Mousavi, J. Bobacka, Coulometric response of solid-contact anion-sensitive electrodes, Electrochim. Acta 367 (2021) 137566. https://doi.org/10.1016/J.ELECTACTA.2020.137566.
[40] T. Forrest, E. Zdrachek, E. Bakker, Thin Layer Membrane Systems as Rapid Development Tool for Potentiometric Solid Contact Ion-selective Electrodes, Electroanalysis 32 (2020) 799–804. https://doi.org/10.1002/ELAN.201900674.
[41] M. Guzinski, J.M. Jarvis, P. D'Orazio, A. Izadyar, B.D. Pendley, E. Lindner, Solid-Contact pH Sensor without CO2 Interference with a Superhydrophobic PEDOT-C14 as Solid Contact: The Ultimate "water Layer" Test, Anal. Chem. 89 (2017) 8468–8475. https://doi.org/10.1021/acs.analchem.7b02009.
[42] M. Guzinski, J.M. Jarvis, F. Perez, B.D. Pendley, E. Lindner, R. De Marco, G.A. Crespo, R.G. Acres, R. Walker, J. Bishop, PEDOT(PSS) as Solid Contact for Ion-Selective Electrodes: The Influence of the PEDOT(PSS) Film Thickness on the Equilibration Times, Anal. Chem. 89 (2017) 3508–3516. https://doi.org/10.1021/acs.analchem.6b04625.
[43] J. Zhao, S. Xu, K. Tschulik, R.G. Compton, M. Wei, D. O'Hare, D.G. Evans, X. Duan, Molecular-scale hybridization of clay monolayers and conducting polymer for thin-film supercapacitors, Adv. Funct. Mater. 25 (2015) 2745–2753. https://doi.org/10.1002/adfm.201500408.
[44] W. Shi, Q. Yao, S. Qu, H. Chen, T. Zhang, L. Chen, Micron-thick highly conductive PEDOT films synthesized via self-inhibited polymerization: roles of anions, NPG Asia Mater. 9 (2017) e405–e405.

https://doi.org/10.1038/am.2017.107.
[45] M. Fu, G. Shi, F. Chen, X. Hong, Doping level change of polythiophene film during its electrochemical growth process, Phys. Chem. Chem. Phys. 4 (2002) 2685–2690. https://doi.org/10.1039/b201041k.
[46] M. Culebras, C.M. Gómez, A. Cantarero, Enhanced thermoelectric performance of PEDOT with different counter-ions optimized by chemical reduction, J. Mater. Chem. A 2 (2014) 10109–10115. https://doi.org/10.1039/c4ta01012d.
[47] S. Garreau, G. Louarn, J.P. Buisson, G. Froyer, S. Lefrant, In Situ Spectroelectrochemical Raman Studies of Poly(3,4-ethylenedioxythiophene) (PEDT), Macromolecules 32 (1999) 6807–6812. https://doi.org/10.1021/ma9905674.
[48] S. Garreau, J.L. Duvail, G. Louarn, Spectroelectrochemical studies of poly(3,4-ethylenedioxythiophene) in aqueous medium, Synth. Met. 125 (2001) 325–329. https://doi.org/https://doi.org/10.1016/S0379-6779(01)00397-6.
[49] A. Michalska, A. Gałuszkiewicz, M. Ogonowska, M. Ocypa, K. Maksymiuk, PEDOT films: Multifunctional membranes for electrochemical ion sensing, J. Solid State Electrochem. 8 (2004) 381–389. https://doi.org/10.1007/s10008-003-0459-8.
[50] Y. Umezawa, K. Umezawa, H. Sato, Selectivity coefficients for ion-selective electrodes: Recommended methods for reporting $K_{A,B}^{pot}$ values (Technical Report), Pure Appl. Chem. 67 (1995) 507–518. https://doi.org/10.1351/PAC199567030507.
[51] K.P. Xiao, P. Bühlmann, S. Nishizawa, S. Amemiya, Y. Umezawa, A Chloride Ion-Selective Solvent Polymeric Membrane Electrode Based on a Hydrogen Bond Forming Ionophore, Anal. Chem. 69 (1997) 1038–1044. https://doi.org/10.1021/ac961035d.
[52] P.C. Meier, W.E. Morf, M. Läubli, W. Simon, Evaluation of the optimum composition of neutral-carrier membrane electrodes with incorporated cation-exchanger sites, Anal. Chim. Acta 156 (1984) 1–8. https://doi.org/10.1016/S0003-2670(00)85531-2.
[53] R. Eugster, P.M. Gehrig, W.E. Morf, U.E. Spichiger, W. Simon, Selectivity-Modifying influence of Anionic Sites in Neutral-Carrier-Based Membrane Electrodes, Anal. Chem. 63 (1991) 2285–2289. https://doi.org/10.1021/ac00020a017.
[54] M. Fibbioli, W.E. Morf, M. Badertscher, N.F. De Rooij, E. Pretsch, Potential drifts of solid-contacted ion-selective electrodes due to zero-current ion fluxes through the sensor membrane, Electroanalysis 12 (2000) 1286–1292. https://doi.org/10.1002/1521-4109(200011)12:16<1286::AID-ELAN1286>3.0.CO;2-Q.
[55] J. Bobacka, A. Lewenstam, A. Ivaska, Equilibrium potential of potentiometric ion sensors under steady-state current by using current-reversal chronopotentiometry, J. Electroanal. Chem. 509 (2001) 27–30. https://doi.org/10.1016/S0022-0728(00)00515-5.
[56] A.R.L. Fraga, J.C. Quintana, G.L. Destri, N. Giamblanco, R.G. Toro, F. Punzo, Polymeric membranes conditioning for sensors applications: Mechanism and influence on analytes detection, J. Solid State Electrochem. 16 (2012) 901–909. https://doi.org/10.1007/S10008-011-1456-Y.
[57] M. Rich, L. Mendecki, S.T. Mensah, E. Blanco-Martinez, S. Armas, P. Calvo-Marzal, A. Radu, K.Y. Chumbimuni-Torres, Circumventing Traditional Conditioning Protocols in Polymer Membrane-Based Ion-Selective Electrodes, Anal. Chem. 88 (2016) 8404–8408. https://doi.org/10.1021/acs.analchem.6b01542.
[58] P. Damala, E. Zdrachek, T. Forrest, E. Bakker, Unconditioned Symmetric Solid-Contact Electrodes for Potentiometric Sensing, Anal. Chem. 94 (2022) 11549–11556. https://doi.org/10.1021/ACS.ANALCHEM.2C01728.
[59] S.M. Armas, A.J. Manhan, O. Younce, P. Calvo-Marzal, K.Y. Chumbimuni-Torres, Ready-to-use single-strip paper based sensor for multiplex ion detection, Sensors Actuators, B Chem. 255 (2018) 1781–1787. https://doi.org/10.1016/j.snb.2017.08.194.
[60] A.C. Lazanas, M.I. Prodromidis, Electrochemical Impedance Spectroscopy–A Tutorial, ACS Meas. Sci. Au 3 (2023) 162–193. https://doi.org/10.1021/ACSMEASURESCIAU.2C00070.
[61] Z. Mousavi, A. Teter, A. Lewenstam, M. Maj-Zurawska, A. Ivaska, J. Bobacka, Comparison of Multi-walled Carbon Nanotubes and Poly(3-octylthiophene) as Ion-to-Electron Transducers in All-Solid-State Potassium Ion-Selective Electrodes, Electroanalysis 23 (2011) 1352–1358. https://doi.org/10.1002/ELAN.201000747.
[62] J. Bobacka, A. Lewenstam, A. Ivaska, Electrochemical impedance spectroscopy of oxidized poly(3,4-ethylenedioxythiophene) film electrodes in aqueous solutions, J. Electroanal. Chem. 489 (2000) 17–27. https://doi.org/10.1016/S0022-0728(00)00206-0.
[63] J. Bobacka, Conducting polymer-based solid-state ion-selective electrodes, Electroanalysis 18 (2006) 7–18. https://doi.org/10.1002/elan.200503384.
[64] Y. Sulaiman, Characterisation of PEDOT and its derivatives in electrochemical sensing applications, Durham University, 2012. http://etheses.dur.ac.uk/3541/.
[65] A.W. Gan, G.E.K.K. Seah, L.H. Kwek, S.S. Goh, Ion transfer voltammetry of amino acids with an all-solid-state

ion-selective electrode for non-destructive phenylalanine sensing, Electroanalysis 35 (2023) e202200501. https://doi.org/10.1002/ELAN.202200501.
[66] Y. Gokdemir, B.T. Karadag, Sweat Testing and Recent Advances, Front. Pediatr. 9 (2021) 1–8. https://doi.org/10.3389/fped.2021.649904.